Field- and temperature-dependent surface resistance of superconducting polycrystalline multiple-phase Hg-Ba-Ca-Cu-O: Evidence for dirty-limit behavior

H. A. Blackstead and D. B. Pulling
Department of Physics, University of Notre Dame, Notre Dame, Indiana 46556

M. Paranthaman and J. Brynestad
Chemistry Division, Oak Ridge National Laboratory, Oak Ridge, Tennessee 37831
(Received 14 October 1994)

Field- and temperature-dependent surface resistance measurements at 12.9 GHz are reported for polycrystalline Hg-Ba-Ca-Cu-O, which was found to consist primarily of the $HgBa_2CaCu_2O_{6+\delta}$ and $HgBa_2Ca_2Cu_3O_{8+\delta}$ phases. A small amount of a third phase, most likely $HgBa_2Ca_3Cu_4O_{10+\delta}$, was also detected. With variation of the angle Ψ between the applied field and current density, the low-temperature data exhibit large flux-flow resistivity that varies approximately as $\sin^2(\Psi)$, while at high temperatures, the dominant field- and temperature-dependent response is attributed to isotropic phase-slip losses in intragranular defects. For temperatures just below the transition temperature of the two-layer phase, very small flux flow is evidenced. This result is consistent with an effective H_{c2} of unusual size, suggesting a dirty-limit value for H_{c2}.

I. INTRODUCTION

In a recent paper, Thompson *et al.*[1] successfully applied the theories of Bulaevskii, Ledvij, and Kogan,[2] and Kogan *et al.*[3] describing the impact of vortex fluctuations on the magnetization of Hg based high-temperature superconductors. As a result, these authors were able to obtain information relating to the temperature dependence of the London penetration depth, the upper critical field H_{c2}, and the coherence length ξ. In this paper, we explore the field and temperature dependence of the high-frequency surface resistance, which is sensitive to these parameters. Interpretation of the data suggests that microsyntactical intergrowth gives rise to a sort of "dirty limit" enhancement of the critical field H_{c2}, significantly reducing the flux-flow losses in the lower transition temperature two-layer phase $HgBa_2CaCu_2O_{6+\delta}$.

The surface resistance, R_s, although a less intuitive probe of the resistivity than direct resistivity measurements, is frequently less limited than dc resistivity measurements in revealing the role of multiple phases,[4] and perhaps more importantly, the manifestation of pinning.[5] Understanding pinning is of immediate importance to the potential application of these materials. Microwave frequency fluxon response amplitudes are *very* small,[6] as compared to macroscopic flux displacements encountered in dc or in low audio frequency measurements. As a consequence, the motion of fluxons in response to Lorentz forces is approximately equivalent to the response of unpinned fluxons, even if the fluxons are effectively pinned at dc or low audio frequencies. It is also the case that nonrectilinear percolative current paths which may be expressed in dc experiments, may cause a "smearing" of the Lorentz force angular dependence, tending to obscure the roles of different dissipation modes. In the case of the contactless microwave frequency experiments in which resonant cavities are employed, the current path in the sample depends on the spatial homogeneity of the rf magnetic field which induces the surface currents. For rectangular resonant cavities, single low-order modes are employed; this results in rectilinear current paths, even in somewhat irregular or polycrystalline samples which are typically much smaller than the microwave wavelength ($\sim$2 cm) in the present case. As a consequence, the microwave experiments are effective in their ability to "sort out" a number of effects. This will be illustrated by the angular dependencies of an electron spin resonance signal, arising from uncoupled Cu 3*d* electrons, and the angular dependence of the "conventional" Bardeen-Stephen flux flow,[7] which is particularly evident in the low-temperature data. At high temperatures, near the transition temperature, the angular dependent surface resistance is dominated by an isotropic dissipation whose origin is attributed to an axially symmetric phase-slip loss arising from defected Cu-O planes which are thought to form nanoscale intragranular Josephson junctions.[8–11] Theoretical models for the surface resistance, particularly for high-temperature superconductors, remain controversial; in this paper we will explore the Coffey-Clem[12–14] model, and introduce a variation of that model which features a different expression for the vortex resistivity which, in a limiting form, has been shown able to describe the dc resistivity of a variety of high-temperature superconducting materials. In the limit of a defectless material, the resistivity model reduces to conventional flux flow. One of the consequences of this modification is that the field-dependent flux-flow response will exhibit a "renormalized" character which leads to a field-dependent maximum in the difference between the "maximum Lorentz force" (MLF) and the "zero Lorentz force" (ZLF) field-current configuration responses. The two-phase character of the

material required the combination of several parameters to form an effective medium theory capable of describing the results. One of the primary interesting features of the data is very small conventional flux-flow response for temperatures just below the transition temperature of the two layer phase. These results are in contrast to the relatively large flux-flow responses observed for temperatures just below the transition temperature of the three layer phase, and the composite response observed at low temperatures. The suppression of the flux flow is attributed to a sort of "dirty limit" value for the composite upper critical field.

II. EXPERIMENT

Polycrystalline Hg-Ba-Ca-Cu-O samples were prepared by the following procedure: the precursor pellets of $Ba_2Ca_2CuO_7$ and Hg reservoir pellets of HgO mixed with $Ba_2Ca_2CuO_7$ precursors were sealed together in a quartz tube and heated to 860 °C, held at 860 °C for 5 h and slow cooled. The details of the procedure were reported elsewhere.[15] Samples were cut into thin rectangular slabs with typical dimensions of $1\times1\times0.1$ mm^3. The samples were mounted, using silicone vacuum grease, to the end wall of a TE_{101} resonant cavity. The samples were covered with a thin coat of this grease which we found reduced their tendency to decompose in humid air. Once installed in the cavity, they were exposed only to inert (helium) gas, and kept below 180 K. These precautions were important, as it was observed that unprotected surfaces decomposed rapidly when exposed to room-temperature humid air. The applied field, variable to a maximum of 1.9 T, was applied in the plane of the sample, and could be rotated in that plane. The power input to the cavity was maintained at a fixed level, typically $\sim$150 mW, giving rise to an rf field amplitude $\sim$0.1 G. The temperature was controlled using helium gas flow, and a heater which is integral to the cavity assembly. Temperature set points were held within errors of $\sim$10 mK during field sweeps through use of a temperature sensitive capacitance thermometer.

III. EXPERIMENTAL RESULTS

In Fig. 1, temperature induced changes in the surface resistance are illustrated using an rf frequency of 12.9 GHz. The data unambiguously indicate two transitions; the high-temperature phase has a transition temperature $T_c^{(1)}$ of approximately 134.5 K, while the lower transition, $T_c^{(2)}$, occurs at approximately 120 K. There is an indication of a third phase at approximately 125 K, although the signal it yields is of such relative size suggesting a much smaller fraction.

Figure 2 summarizes the observed changes in the surface resistance with the applied field parallel to the rf current density in the sample plane. In this configuration, the rf magnetic field is perpendicular to the static field, satisfying the requirements for electron spin resonance. It is evident that there is a significant number of unpaired paramagnetic copper $3d$ electrons, which resonate with an intensity which varies as $1/T$. The two

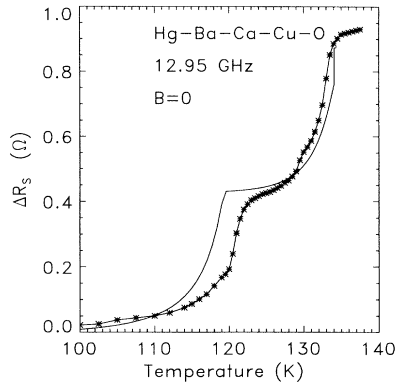

FIG. 1. Temperature induced change in the surface resistance for $B=0$. Two transitions are immediately evident, at approximately 134.5 K ($HgBa_2Ca_2Cu_3O_{8+\delta}$) and 120 K ($HgBa_2CaCu_2O_{6+\delta}$). A small amount of a third phase, most likely $HgBa_2Ca_3Cu_4O_{10+\delta}$ is noticed at approximately 125 K. The solid line is the modeled response, which does not include the small third phase contribution. The data include the temperature-dependent cavity background, which varies smoothly with temperature.

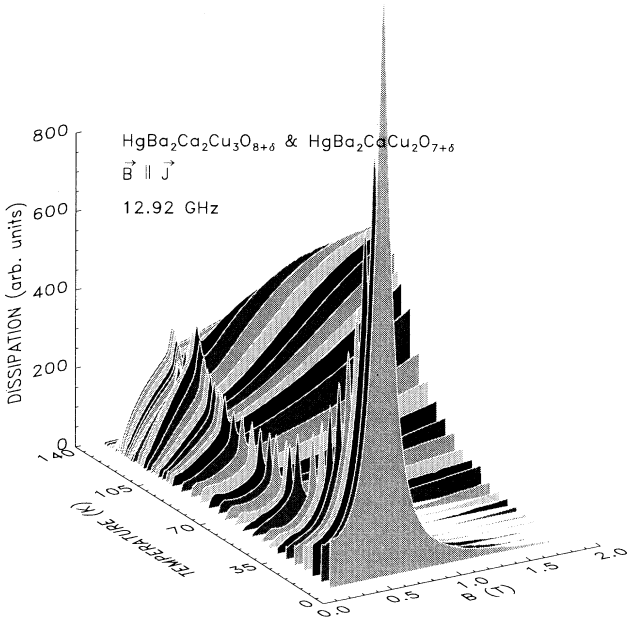

FIG. 2. Temperature dependence of field induced changes in the surface resistance of polycrystalline two phase Hg-Ba-Ca-Cu-O. The high-temperature three layer phase, $HgBa_2Ca_2Cu_3O_{8+\delta}$, exhibits an onset temperature of 134.5 K, while the two layer phase, $HgBa_2CaCu_2O_{6+\delta}$, is evident at 120 K. In this case, the field is applied parallel to the current in the zero Lorentz force configuration. At low temperatures, the dissipation is dominated by an electron spin resonance due to Cu spins, since in the ZLF configuration the rf magnetic field is perpendicular to the applied field. The field induced changes, proportional to ΔR_s, are systematically smaller than for the maximum Lorentz configuration data illustrated in Fig. 3.

major phases are evidenced by large changes in the field-dependent response at temperatures just below the onset temperatures $T_c^{(1)}=134.5$ K and $T_c^{(2)}=120$ K.

Data with the rf current perpendicular to the field are illustrated in Fig. 3. In these data, the electron spin resonance is greatly attenuated. If the rf field were perfectly aligned parallel to the dc field, the resonance would be expected to vanish. The data suggest a field misalignment of $\sim 1°$. The responses observed in this configuration are of the same order of magnitude as those in Fig. 2. It is important to note that the near vanishing of the electron spin resonance confirms the spatial homogeneity of the rf magnetic field, and by Ampere's law, the induced rf current density. Thus the large responses observed in Fig. 2 are *not* due to percolative or meandering current paths in the sample surface. This behavior is not unusual, as it has previously been reported for melt-textured[16] Gd-Ba-Cu-O. The applied fields are also too large to expect any impact of flux entanglement.[17–20]

Two field scans, with **B** parallel and perpendicular to the current density at 130.5 K are illustrated in Fig. 4. The difference of these scans is also given. The electron spin resonance is clearly evidenced in the parallel configuration, but is not observed in the perpendicular scan, confirming the rectilinear character of the rf magnetic field and the induced current density. The difference of these scans, due to flux flow, exhibits a maximum at an applied field of approximately 0.8 T. This maximum is a consequence of the "renormalization" of the flux flow by the phase-slip resistivity. This results because the phase-slip resistivity increases more rapidly with applied field than does the flux-flow contribution. This feature will be treated below in some detail.

The data in Fig. 5 result from rotations of the applied field in the *a-b* plane, at a fixed field of 1 T, as a function of temperature. For temperatures very close (as $T\rightarrow T_c$ from below) to the highest transition temperature, $T_c^{(1)}$, the rotation data tend to be isotropic, as the phase-slip

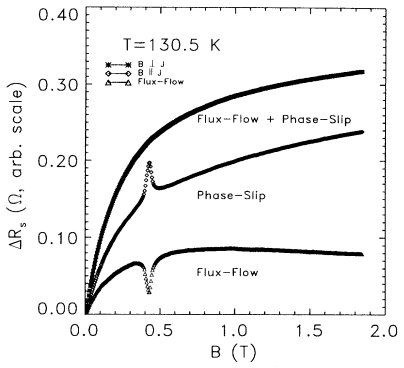

FIG. 4. Field-dependent responses at $T=130.5$ K with the applied field parallel and perpendicular to the rf current. Also illustrated is the difference between these two signals. The difference, which may be attributed to flux flow, exhibits a maximum at approximately 1 T. These data illustrate the renormalization of the response which phase-slip resistivity provides. This results because the phase-slip and the flux-flow contributions have different field (and temperature) dependencies.

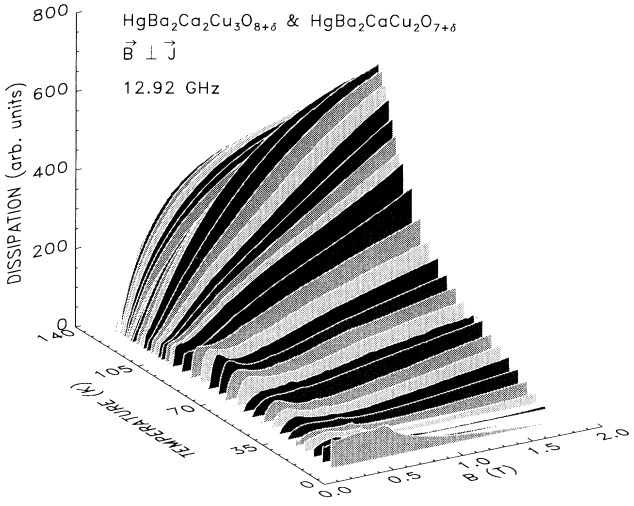

FIG. 3. Temperature dependence of field induced changes in dissipation proportional to ΔR_s, with **B⊥J** in the maximum Lorentz force configuration. Here, the electron spin resonance is noticeable only at the lowest temperatures, and may have resulted from less than $\frac{1}{2}°$ field misalignment. The data in this case (plotted to the same scale as in Fig. 2) although systematically larger than those of Fig. 2 are the *same* magnitude, except at the field for the electron spin resonance. The dramatic difference in the resonant response is characteristic of a unidirectional rf magnetic field, which as a consequence of Ampere's law produces a perpendicular rf current density in the sample plane.

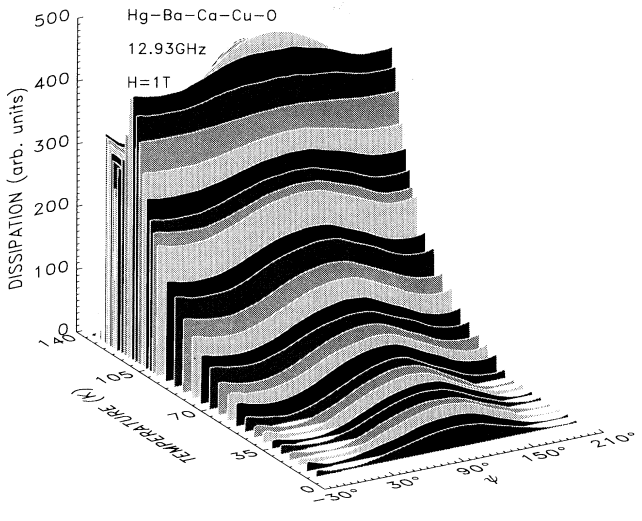

FIG. 5. Field induced changes in the dissipation resulting from rotations of the applied field in the sample plane relative to the current direction in a fixed field of 1 T. Near each transition temperature, the response tends to be isotropic, with a superimposed angular dependent response which is proportional to $\sin^2(\Psi)$, and vanishes as the onset temperature is approached. At low temperatures, the isotropic response is greatly reduced, and the $\sin^2(\Psi)$ response which is due to flux flow is dominant.

resistivity renormalization dominates the flux-flow contribution. This behavior is both typical for high-temperature materials, and in contradiction to models for the surface resistance which include flux flow or flux creep as the only dissipation mechanism. Such models generally lead to a maximum in the fixed field rotational response at the onset temperature, or more precisely at $T_c(\mathbf{B})$.

A specific angular-dependent response in the high-temperature phase is illustrated in Fig. 6, at $T=130.5$ K. The data reveal a response which is accurately proportional to $\sin^2(\Psi)$ added to a constant b. The isotropic "background" (b) is attributed to the phase-slip resistivity, which is dominant. Here, the data were scaled by a constant factor, a consequence of the feature that the microwave system employed is not easily calibrated. The solid white line is the computed response. With a conventional flux-flow model, the angular dependent response would be described with $b\sim 0$, since the dissipation would tend to vanish in the ZLF configuration.

In Fig. 7, the data over a limited temperature range emphasizing the transition region for the highest temperature phase at a fixed field $B=1$ T with both $\Psi=0$, and $\pi/2$ is illustrated along with the modeled surface resistance changes (solid lines) as given by the Coffey-Clem model with no junction contribution. It is evident that the model in this limit does not provide an accurate representation of the data. The temperature-dependent response at a fixed field $B=1$ T with both $\Psi=0$ and $\pi/2$ is illustrated in Fig. 8, over the full temperature range of interest; the solid lines are model computations which include a contribution from junctions. This model fails to describe the data near $T=125$ K because it includes the contributions from only the two dominant phases. These data emphasize the near vanishing of the flux-flow response for T near 115 K. It is also evident that the flux-flow contribution of the three layer phase is comparatively quite large, for temperatures several degrees below $T_c^{(1)}$. With the exception of temperatures near 115

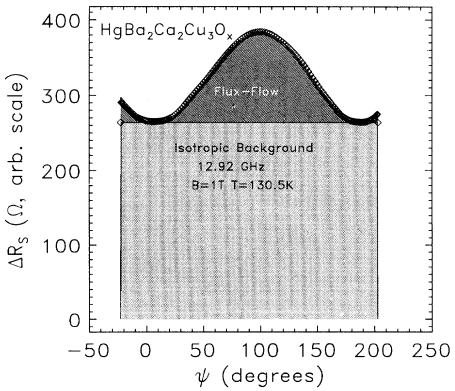

FIG. 6. Angular dependent response with $\mathbf{B}=1$ T at 130.5 K, for the high-temperature phase. The data indicate a large isotropic signal with a superimposed flux-flow response which varies closely as $\sin^2(\Psi)$. The solid white line is the computed response, and the experimental data were scaled by a constant factor.

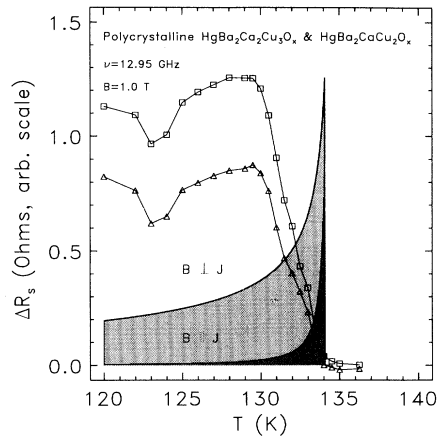

FIG. 7. Unmodified Coffey-Clem model computations for the field-induced change ΔR_s at a fixed maximum field $\mathbf{B}=1$ T are illustrated over a limited temperature range, showing the narrow temperature-dependent response typical of a flux-flow model. The response computed for $\mathbf{J}\|\mathbf{B}$ was multiplied by a factor of 10^4; the data for both orientations were scaled by a constant factor selected to make the peak heights of the $\mathbf{B}\perp\mathbf{J}$ configurations match. The unavoidable conclusions are that λ_β is far too small, the flux-flow response varies too rapidly as a function of temperature, and the model does not describe the $B=0$ transition width. The data here and in Fig. 1 give a transition width of approximately 5 K.

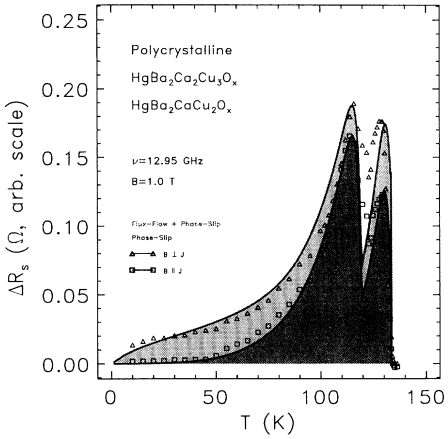

FIG. 8. Temperature dependence of the field-induced change ΔR_s at a fixed maximum field $\mathbf{B}=1$ T with the field parallel and perpendicular to the rf current. The data clearly reveal the two phases, as indicated by the rapid rise in the dissipation at temperatures corresponding to the transition temperatures. The fits are indicated by the solid lines. For temperatures $T_c^{(2)}<T<T_c^{(1)}$, the data show a large difference between the ZLF and MLF field-current configurations. This is in *contrast* to the data for T near but below $T_c^{(2)}$. In this region, the data indicate a near vanishing of flux flow, accompanied with a large phase-slip contribution. This reduction is a consequence of a large effective H_{c2} and large phase-slip renormalization. The fits (using one set of parameters) fail to describe the data in a small temperature range near 125 K. This is due to a small concentration of a third phase, most probably four-layer $HgBa_2Ca_3Cu_4O_{10+\delta}$.

K, this model, including the junction contributions, describes all trends and details with considerable accuracy. The model is discussed in detail in the following section.

IV. ANALYSIS

Following Coffey and Clem, the surface resistance R_s is expressed in terms of two complex penetration depths, $\lambda_\gamma = \lambda_{1\gamma} + i\lambda_{2\gamma}$ and $\lambda_\beta = \lambda_{1\beta} + i\lambda_{2\beta}$,

$$R_s = \omega\mu_0\{\sin^2(\Psi)\lambda_{2\gamma} + \cos^2(\Psi)\lambda_{2\beta}\} , \tag{1}$$

with ω the angular microwave frequency, B the applied field, T the temperature, and Ψ the angle between the applied field and the rf current density in the sample plane. The several relationships are defined:

$$\lambda_\gamma^2(\omega,B,T,\varphi) = \{\lambda^2(B,T) + (i/2)[\delta_{vf}^2(B,T,\omega) + \delta_{vj}^2(B,T,\omega,J)]\} / \{1 - 2i\lambda^2(B,T)/\delta_{nf}^2(B,T,\omega)\} , \tag{2}$$

$$\lambda_\beta^2(\omega,B,T) = \{\lambda^2(B,T) + (i/2)[\delta_{vf}^2(B,T,\omega)\cos^2(\theta) + \delta_{vj}^2(B,T,\omega,J)]\} / \{1 - 2i\lambda^2(B,T)/\delta_{nf}^2(B,T,\omega)\} , \tag{3}$$

$$\delta_{nf}^2(\omega,B,T) = (2\rho_n/\mu_0\omega)/\{1 - [1 - (T/T_c)^4][1 - B/(H_{c20}[1 - (T/T_c)^2]/[1 + (T/T_c)^2])]\} , \tag{4}$$

$$\lambda(T) = \lambda(0)/(1 - T/T_c)^{1/2} , \tag{5}$$

$$\mu(\omega,T) = 1/\eta\{1 + [-i\omega\eta/\alpha\kappa_{\rho 0} + 1/(I_0^2[U(1 - T/T_c)^{3/2}/B] - 1)]^{-1}\}^{-1} , \tag{6}$$

$$\rho_{ff}(\omega) = B\varphi_0\mu(\omega,T) , \tag{7}$$

$$\eta = \varphi_0 H_{c2}/\rho_n , \tag{8}$$

$$\delta_{vf}^2(B,T,\omega) = 2\rho_{ff}(B,T,\omega)/\mu_0\omega , \tag{9}$$

$$\delta_{vj}^2(B,T,\omega,J) = 2\rho_{ps}(B,T,J)/\mu_0\omega . \tag{10}$$

Here $\kappa_{\rho 0}$ is the force constant to the pinning potential, $\alpha = I_1(\nu)/I_0(\nu)$, where I_p is a modified Bessel function with $\nu = U(1 - T/T_c)^{3/2}/B$. For a field in the sample plane, $\theta = \pi/2$. The results are very insensitive to $\kappa_{\rho 0}$ and U, provided that $\kappa_{\rho 0}$ is small, and U is finite. It is important to note that in the limit for which $\kappa_{\rho 0} \to 0$, $\mu = 1/\eta$, and $\rho_v(\omega) = \rho_n B/H_{c2}$. In this limit, the Coffey-Clem theory simplifies to a two fluid model including a combination of conventional flux flow, and effects due to the London penetration depth. Results for typical parameters are included in Fig. 7 for B parallel and perpendicular to the rf current density. The several constants employed in evaluating these functions are given in Table I. It is clear that this model *does not* yield an accurate description of the experimental results, *particularly* for $\Psi = 0$ with $\mathbf{B} \| \mathbf{J}$. For this case, the shape of the response is very different, and the amplitude is *several* orders of magnitude too small. Including the features described with finite $\kappa_{\rho 0}$ leads to a *smaller* computed response. The results of Bonn *et al.*[21] are of particular relevance. These authors carried out both dc measurements of the resistivity, and surface resistance measurements on the same sample of Y-Ba-Cu-O. Their results were that the $B = 0$ transition region could be described with *considerable* accuracy by computing the conventional classical surface resistance $R_s = [\omega\mu_0\rho(T)/2]^{1/2}$. Thus the surface resistance was shown to be a *reliable* indicator of the dc transition width. By obvious extension, near the transition temperatures, we might expect the field broadened surface resistance to be dominated by dc resistivity effects. The Coffey-Clem theory does not include a model for a finite dc transition width; as a result, $\Delta R_s/\Delta T$ is overestimated. In a recent paper, Yeh *et al.*[22] employed the Coffey-Clem model for modeling of high field surface resistance data, but used the Ambegaokar-Baratoff[23] model for $B = 0$. Losses in the grain boundary junctions treated for $B = 0$ were ignored for $B > 0$. The $B = 0$ model employed by these authors was not extended to include field dependence. The model we employ, in a modification of the vortex resistivity, also has its origin in intrinsic junctions. Since H_{c20} for the Nd-Ce-Cu-O is ~ 8 T, the high field surface resistance data of Yeh *et al.* could be expected to be dominated by flux-flow effects, as described by Coffey-Clem. Yeh did not include data for small B, or data with $\mathbf{B} \| \mathbf{J}$ in the ZLF configuration. In order to effectively describe the data reported here, which are typical of polycrystalline materials, it was necessary to extend the resistivity model included in the Coffey-Clem analysis, which incorporates conventional flux flow and flux creep, with a phenomenological model which is capable of describing the dc resistivity of these materials including the $B = 0$ transition width. Several different expressions have been given for the resistivity with $T < T_c$, and $B > 0$: these include the Geshkenbein *et al.*[24] and Vinocur *et al.*[25] (GV) form, the flux-creep model of Krause,

TABLE I. Superconducting parameters obtained from the surface resistance model for polycrystalline multiphase Hg-Ba-Ca-Cu-O.

T_c (K)	H_{c20} (T)	A_T (T)	B_0 (T)	$\lambda(T=0)$ (μm)	$\rho(T_c)$ ($\mu\Omega$ m)
134.5	320	4150	0.33	0.12	15.0
119.5	620	6350	0.35	0.12	15.0

Shi, and Datars[26] (KSD) and the Tinkham[27,28] form as modified and described by Blackstead,[29] and Blackstead *et al.*[30,31] (TB). Each of these models includes inverse fractional B power law dependence. However, the GV and KSD models are only able to describe the experimental data in the limits of fields and low temperatures for which $\rho(B,T)/\rho(B=0,T=T_c)<10^{-2}$. The regions excluded by these two models are precisely those illustrated by the data given here, and the region which Bonn *et al.* discussed. In addition, the GV and KSD models would not be expected to give finite resistivities with $\mathbf{B}\|\mathbf{J}$, in the ZLF configuration. As a consequence, we adopt a *phenomenological* model for the junction contribution $\delta_{vj}^2(B,T,J)=2\rho_{ps}(B,T,J)/\mu_0\omega$ which has its origin in small intrinsic junctions, and provides for an axially symmetric resistivity, and a finite transition width. Lee and Stroud[32] have demonstrated that a network of junctions, with an applied field, gives rise to finite resistivity even with $\mathbf{B}\|\mathbf{J}$, as a consequence of frustration effects. They have compared their model computations to the experimental results of Kwok *et al.*, and demonstrated *qualitative* agreement with the data. Previously, it had been shown that the model given here, with $\beta=1$, yielded a *quantitative* description of the same data. Since the equations employed by Lee and Stroud did not explicitly include Lorentz forces, it may be concluded that the force equation employed by Coffey and Clem describes a different dissipation mechanism. In the limit for which the parameter A_T (the Tinkham constant) is large, the junction contribution surface resistance $\delta_{vj}^2(B,T,J)$ vanishes, and this model reduces exactly to the simplified Coffey-Clem model, with its very small transition width. This revised form of the vortex resistivity allows for a nearly isotropic (planar) surface resistance under particular circumstances. The TB model[33] has also been applied successfully to the description of resistivity data for polycrystalline Tl-Ca-Ba-Cu-O in the ZLF configuration in applied fields varying to a maximum of 25 T for a wide range of temperatures, including the temperature region near the transition temperature which, as mentioned, is not within the domain of either the GV or KSD models. With

$$\gamma=A_T(1-T/T_c)^{3/2}(1-J/J_{c0})^{3/2}/(B+B_0)\ , \tag{11}$$

the axially symmetric phase slip resistivity is given by

$$\rho_{ps}=\rho_n/[I_0(\gamma^\beta/2)]^2\ . \tag{12}$$

Here ρ_n is the temperature-dependent normal resistivity, J_{c0} is the critical current density, and $\beta=\frac{1}{3}$. For Y-Ba-Cu-O, $\beta=1$. In the following, we will ignore the current dependence. Kapustin *et al.*[34] demonstrated that the unmodified Tinkham model ($\beta=1$) did not describe the data they provided; the modified form with $\beta=\frac{1}{3}$ and including B_0, does provide a detailed description of the Kapustin data, which were obtained with $\mathbf{B}\|\mathbf{J}$ in the ZLF configuration. The parameter B_0 is included to describe the $B=0$ transition width; the phase slip resistivity would also give nonphysical results for small fields.

For a two-phase material with microsyntactic intergrowth, it is necessary to combine several lengths. If the sample consisted of large or well separated (samples often have Meissner fractions <1) crystallites, a superposition of the resistivities of each phase might render a good description of the data, but that was found not to work for this material. Two features prevented this simpler approach from working. The flux flow observed in the rotations almost vanishes for temperatures just below the lower transition: this could not occur with a simple superposition as the (modeled) flux-flow contribution arising from the high-temperature phase alone greatly exceeds the observed response. The data show a very large (unusually) flux-flow response which if it were described with single material parameters, the value for H_{c2} required to fit the data would be anomalously small, and contrary to experiment. As a result, it was found necessary to *combine* several parameters and obtain a model for a composite material. With α the fractional weighting of the high temperature phase,

$$1/\delta_{nf}=\alpha/\delta_{nf}^{(1)}+(1-\alpha)/\delta_{nf}^{(2)}\ , \tag{13}$$

$$1/\lambda=\alpha/\lambda^{(1)}+(1-\alpha)/\lambda^{(2)}\ . \tag{14}$$

The critical field H_{c2} varies as $1/\xi^2$, so they are combined as

$$H_{c2}=\{\alpha(H_{c2}^{(1)})^{1/2}+(1-\alpha)(H_{c2}^{(2)})^{1/2}\}^2\ . \tag{15}$$

The data indicate that the phase-slip contributions add directly; accordingly the phase-slip resistivity is given by

$$\rho_{ps}=\alpha\rho_{ps}^{(1)}+(1-\alpha)\rho_{ps}^{(2)}\ . \tag{16}$$

The renormalized flux flow is expressed as

$$\rho_{ff}(B,T)=[\rho_n-\rho_{ps}(B,T,J)]B/H_{c2}(T)\ . \tag{17}$$

In this approach, the total resistivity is given by

$$\rho_t=\rho_{ff}+\rho_{ps}\ . \tag{18}$$

The assumed form of vortex resistivity implicitly includes an important frequency-dependent feature not usually observed at low (audio) frequencies. The flux-flow contribution, as identified explicitly by $\sin^2$ dependence on the angle between the current density and the applied field, is *rarely* observed in dc measurements; for an example, see Kwok *et al.*[35] This is a consequence of pinning; at microwave frequencies, the fluxon vibration amplitude is so small that fluxons may be constrained to sit in a pinning center, and yet will appear to be unpinned. The fitting yielded $\alpha=0.69$; all other parameters are included in Table I. The composition phase-slip resistivity provides an effective renormalization of the flux flow for both phases, and the composite H_{c2} for temperatures $<T_c^{(2)}$ is quite large, effectively limiting the flux-flow response, in a good approximation of the observed response for temperatures of approximately 115 K. This renormalization is evident in the data, and appears to be a common feature of surface resistance measurements for temperatures within a few degrees of the transition temperature. This form of renormalization is required to prevent the addition of two resistivities from exceeding the temperature-dependent normal resistivity in the superconducting state; exceeding the normal state resistivi-

ty would be nonphysical. The normal state resistivity was assumed to vary linearly with temperatures as $\rho_n(T)=(0.9T/T_c+0.1)\rho(T_c)$. This assumes a small residual resistivity at $T=0$.

V. DISCUSSION

The model for the surface resistance presented above has been shown to describe the data with reasonable (if not surprising) fidelity. In particular, the unusual features of the surface resistance data on this polycrystalline material compelled the construction of a model for a composite response. These two demanding features were the large flux flow in the three layer component, which has the highest transition temperature, and the remarkably small flux-flow signature observed for temperatures just below the transition temperature of the two layer phase. Some evidence for a third phase (probably the four-layer variant) was also obtained, but the relative concentration of this phase was too small to permit differentiation from the two dominant phases. We emphasize that the flux-flow contribution from the high-temperature phase, treated independently, substantially exceeds the observed response in this temperature range. The impact of the model is to suggest that the microsystactatial intergrowths appear as defects, substantially increasing the effective H_{c2}. While defects are generally considered to be deleterious, this sort of defect actually improves (reduces) the flux-flow losses evidenced. In these layered materials, the short coherence lengths make the introduction of pinning defects a formidable technical objective. Rather, it is indicated by these results that the intergrowth structures lead to approximate dirty limits for both phases. It is an important result to suggest that such defects tend to reduce the flux-flow losses, a useful material design goal. Unfortunately, the corresponding increase in the effective phase-slip losses appear to largely nullify this potential improvement. The size of the fit values for H_{c20} appear to be larger than might be expected from the data of Thompson *et al.* It is easy to show[36] that for a polycrystalline material with large anisotropy, the effective average value observed in flux flow, is $\sim\frac{1}{2}H_{c2}(T)$. As a consequence, for the two and three layer phases, the value for $-dH_{c2}/dT|_{T\approx T_c}\cong 1-2$ T/K, as is typical for high-temperature superconductors.

From a theoretical point of view, we have also demonstrated that simple flux-flow models for dissipative losses in this class of layered materials describe only a small part of the total losses. An axially symmetric loss term, generally required to describe the angular dependent data, is generally not treated. This may result because most researchers do not have the equipment necessary to investigate resistive losses with the ZLF configuration. For a counter example in which the flux-flow losses dominate, the reader is referred to similar measurements on high quality Y-Ba-Cu-O films.[37] The physics required to describe the "junction" dissipative mechanism may also play a role in the origin of the superconductivity of these materials. This is discussed in some detail by Phillips,[38,39] using a model which has not received appropriate attention. Since radiation of apparent junction origin has been observed from several of the layered systems, the existence of small junctions in these materials as a consequence of planar defects can hardly be ignored. Kleiner and Müller[40] have shown by direct measurements that intrinsic Josephson junction effects are exhibited by layered high-temperature superconductors. Their results, which demonstrate that these materials behave like stacks of superconductor-insulator-superconductor Josephson junctions, are consistent with a resistivity model which has been suggested. The model for the axially symmetric resistivity employed here has this model as its origin. In order to clarify the role of anisotropy versus layering, a comparative study of NbN has been undertaken, and will be published elsewhere.[41] The principle result is that NbN films, prepared by pulsed laser deposition, are anisotropic granular or layered materials, which also exhibit axially symmetric dissipative losses similar to those reported here. Kim *et al.*[42] have previously reported axially symmetric resistivity in granular NbN films. We conclude that defected layers give rise to transport parallel to the c axis, most likely as a consequence of Josephson coupling, and are the source of the large axially symmetric surface resistance reported here.

ACKNOWLEDGMENTS

H.A.B. and D.B.P. gratefully acknowledge support from the Midwest Superconducting Consortium through U.S. Department of Energy Grant No. DE-FG02-90ER45427. H.A.B. thanks J.C. Phillips (AT&T), H. Newman (NRL), D. Stroud (Ohio State), M. Coffey (NIST), and J. Clem (Iowa State) for very helpful discussions. M.P. and J.B. acknowledge the support of the work sponsored by the Division of Materials Sciences, Office of Basic Energy Sciences, U.S. Department of Energy and technology development was funded by the U.S. Department of Energy Office of Advanced Utility Concept–Superconductor Technology Program, both under Contract No. DE-AC05-84OR2140 with Martin Marietta Energy Systems, Inc.

[1]J. R. Thompson, J. G. Ossandon, D. K. Christen, B. C. Chakoumakos, Y. R. Sun, M. Paranthaman, and J. Brynestad, Phys. Rev. B **48**, 14 031 (1993).

[2]L. N. Bulaevskii, M. Ledvij, and V. G. Kogan, Phys. Rev. Lett. **68**, 3773 (1992).

[3]V. G. Kogan, M. Ledvij, A. Yu, Simonov, J. H. Cho, and D. C. Johnston, Phys. Rev. Lett. **70**, 1870 (1993).

[4]H. A. Blackstead, D. B. Pulling, and H. Sato, Phys. Status Solidi A **140**, 509 (1993).

[5]H. A. Blackstead, D. B. Pulling, P. J. McGinn, and W. H. Chen, J. Supercond. **4**, 263 (1991).

[6]W. J. Tomasch, H. A. Blackstead, S. T. Ruggiero, P. J. McGinn, John R. Clem, K. Shen, J. W. Weber, and D. Boyne, Phys. Rev. B **37**, 9864 (1988).

[7]J. Bardeen and M. J. Stephen, Phys. Rev. **140**, A1197 (1965).
[8]H. A. Blackstead, J. Supercond. **5**, 67 (1992).
[9]H. A. Blackstead, Solid State Commun. **87**, 35 (1993).
[10]H. A. Blackstead, D. G. Keiffer, M. D. Lan, and J. Z. Liu, Superlatt. Microstruct. **13**, 279 (1993).
[11]H. A. Blackstead, Phys. Rev. B **47**, 11 411 (1993).
[12]M. W. Coffey and J. W. Clem, Phys. Rev. Lett. **67**, 386 (1992).
[13]M. W. Coffey and J. W. Clem, Phys. Rev. B **45**, 10 527 (1992).
[14]J. R. Clem and M. W. Coffey, Physica C **185-189**, 1915 (1991).
[15]M. Parathanaman, Physica C **222**, 7 (1994).
[16]H. A. Blackstead, D. B. Pulling, and C. A. Clough, Phys. Rev. B **47**, 8978 (1993).
[17]D. R. Nelson, Physica C **162-164**, 1156 (1989).
[18]D. R. Nelson, J. Stat. Phys. **57**, 511 (1989).
[19]D. R. Nelson and H. S. Seung, Phys. Rev. B **39**, 9153 (1989).
[20]S. B. Obukhov and M. Rubinstein, Phys. Rev. Lett. **65**, 1279 (1990).
[21]D. A. Bonn, R. Liang, T. M. Riseman, D. J. Baar, D. C. Morgan, K. Zhang, P. Dosanjh, T. L. Duty, A. McFarlane, G. D. Morris, J. H. Brewer, W. N. Hardy, C. Kallin, and A. J. Berlinsky, Phys. Rev. B **47**, 11 314 (1993).
[22]N-C. Yeh, U. Kriplani, W. Jiang, D. S. Reed, D. M. Strayer, J. B. Barner, B. D. Hunt, M. C. Foote, and R. P. Vasques, A. Gupta, and A. Kussmaul, Phys. Rev. B **48**, 9861 (1993).
[23]V. Ambegaokar and A. Baratoff, Phys. Rev. Lett. **10**, 486 (1963).
[24]V. Geshkenbein, A. Larkin, M. V. Feigel'man, and V. Vinocur, Physica C **162-164**, 239 (1989).
[25]V. M. Vinocur, M. V. Feigel'man, V. B. Geshkenbein, and A. I. Larkin, Phys. Rev. Lett. **65**, 259 (1990).
[26]T. W. Krause, A.-C. Shi, and W. R. Datars, Physica C **205**, 99 (1993).
[27]M. Tinkham, Phys. Rev. Lett. **61**, 1658 (1988).
[28]M. Tinkham and C. J. Lobb, in *Solid State Physics,* edited by H. Ehrenreich and D. Turnbull (Academic, New York, 1989), Vol. 42, pp. 91–134.
[29]H. A. Blackstead, Solid State Commun. **87**, 35 (1993).
[30]H. A. Blackstead, D. B. Pulling, D. G. Keiffer, M. Sankararaman, and H. Sato, Phys. Lett. A **170**, 130 (1992).
[31]H. A. Blackstead, D. B. Pulling, and H. Sato, Phys. Status Solidi A **140**, 509 (1993).
[32]K. H. Lee and D. Stroud, Phys. Rev. B **46**, 5699 (1992).
[33]H. A. Blackstead and G. A. Kapustin, Physica C **219**, 109 (1994).
[34]G. A. Kapustin, B. B. Tolkachev, Yu. A. Cherushev, and L. D. Shustov, Physica C **190**, 549 (1992).
[35]W. K. Kwok, U. Welp, G. W. Crabtree, K. G. Vandervoort, R. Hulscher, and J. Z. Liu, Phys. Rev. Lett. **64**, 966 (1990).
[36]H. A. Blackstead, D. B. Pulling, and H. Sato, Phys. Status Solidi A **140**, 509 (1993).
[37]H. A. Blackstead, D. B. Pulling, J. S. Horwitz, and D. B. Chrisey, Phys. Rev. B **49**, 15 335 (1994).
[38]J. C. Phillips, Phys. Rev. B **41**, 8968 (1990).
[39]J. C. Phillips, Phys. Rev. B **46**, 8542 (1992).
[40]R. Kleiner and P. Müller, Phys. Rev. B **49**, 1327 (1994).
[41]H. A. Blackstead, D. B. Pulling, R. E. Treece, J. S. Horwitz, and D. B. Chrisey (unpublished).
[42]D. H. Kim, K. E. Gray, R. T. Kampwirth, K. C. Woo, D. M. McKay, and J. Stein, Phys. Rev. B **41**, 11 642 (1990).

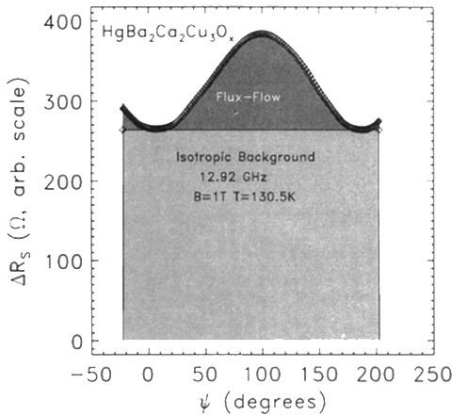

FIG. 6. Angular dependent response with $\mathbf{B}=1$ T at 130.5 K, for the high-temperature phase. The data indicate a large isotropic signal with a superimposed flux-flow response which varies closely as $\sin^2(\Psi)$. The solid white line is the computed response, and the experimental data were scaled by a constant factor.

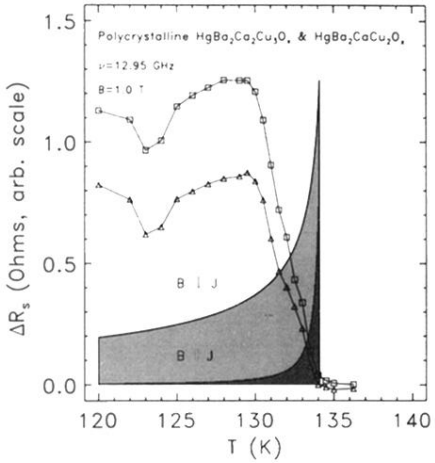

FIG. 7. Unmodified Coffey-Clem model computations for the field-induced change ΔR_s at a fixed maximum field $\mathbf{B}=1$ T are illustrated over a limited temperature range, showing the narrow temperature-dependent response typical of a flux-flow model. The response computed for $\mathbf{J}\|\mathbf{B}$ was multiplied by a factor of 10^4; the data for both orientations were scaled by a constant factor selected to make the peak heights of the $\mathbf{B}\perp\mathbf{J}$ configurations match. The unavoidable conclusions are that λ_β is far too small, the flux-flow response varies too rapidly as a function of temperature, and the model does not describe the $B=0$ transition width. The data here and in Fig. 1 give a transition width of approximately 5 K.

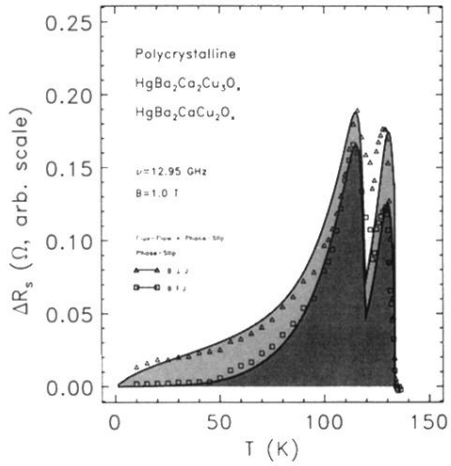

FIG. 8. Temperature dependence of the field-induced change ΔR_s at a fixed maximum field $\mathbf{B}=1$ T with the field parallel and perpendicular to the rf current. The data clearly reveal the two phases, as indicated by the rapid rise in the dissipation at temperatures corresponding to the transition temperatures. The fits are indicated by the solid lines. For temperatures $T_c^{(2)} < T < T_c^{(1)}$, the data show a large difference between the ZLF and MLF field-current configurations. This is in *contrast* to the data for T near but below $T_c^{(2)}$. In this region, the data indicate a near vanishing of flux flow, accompanied with a large phase-slip contribution. This reduction is a consequence of a large effective H_{c2} and large phase-slip renormalization. The fits (using one set of parameters) fail to describe the data in a small temperature range near 125 K. This is due to a small concentration of a third phase, most probably four-layer $HgBa_2Ca_3Cu_4O_{10+\delta}$.